

Proceeding Paper

Fe–Mn Alloys Electroforming Process Using Choline Chloride Based Deep Eutectic Solvents [†]

Vinicius Sales ^{1,2}, Carlo Paternoster ^{1,2}, Diego Mantovani ^{1,2}  and Georgios Kolliopoulos ^{2,*} 

¹ Laboratory of Biomaterials and Bioengineering (LBB), Canada Research Chair Level I in Biomaterials and Bioengineering for Innovation in Surgery, Quebec City, QC G1L 3L5, Canada; vinicius.de-oliveira-fidelis-sales.1@ulaval.ca (V.S.); carlo.paternoster.1@ulaval.ca (C.P.); diego.mantovani@gmn.ulaval.ca (D.M.)

² Department of Mining, Metallurgical, and Materials Engineering, Université Laval, Quebec City, QC G1V 0A6, Canada

* Correspondence: georgios.kolliopoulos@gmn.ulaval.ca

[†] Presented at International Conference on Raw Materials and Circular Economy, Athens, Greece, 5–9 September 2021.

Abstract: Aqueous solvents, despite being effective in the electrodeposition of metals with positive reduction potential, fail to deposit metals with negative reduction potential due to their narrow electrochemical potential window. Deep eutectic solvents (DESs), a class of ionic liquids, are a promising alternative of inexpensive, biodegradable, non-toxic anhydrous solvents that present wide electrochemical potential windows. The present work reports on the potential of choline chloride/ethylene glycol DES in the electrodeposition of Fe–Mn alloys. Cyclic voltammetry tests showed that increasing the quantity of Mn in the bath composition decreases the deposition current of the alloy.

Keywords: sustainable processing; electroforming; deep eutectic solvents; bioresorbable metals



Citation: Sales, V.; Paternoster, C.; Mantovani, D.; Kolliopoulos, G. Fe–Mn Alloys Electroforming Process Using Choline Chloride Based Deep Eutectic Solvents. *Mater. Proc.* **2021**, *5*, 40. <https://doi.org/10.3390/materproc2021005040>

Academic Editor: Konstantinos Simeonidis

Published: 30 November 2021

Publisher's Note: MDPI stays neutral with regard to jurisdictional claims in published maps and institutional affiliations.



Copyright: © 2021 by the authors. Licensee MDPI, Basel, Switzerland. This article is an open access article distributed under the terms and conditions of the Creative Commons Attribution (CC BY) license (<https://creativecommons.org/licenses/by/4.0/>).

1. Introduction

Electroforming is a metal forming and alloying process, whereby thin metal components are fabricated via metal deposition onto a base shape or mold [1]. Once the plated metal layers have been deposited, the newly formed part is stripped off the substrate. This approach presents a sustainable alternative to conventional casting techniques to produce thin-layer alloys with interesting mechanical properties for niche biomedical applications. However, electrodeposition in aqueous solutions has limitations, which are often associated with a simultaneous hydrogen evolution reaction. When metal films are deposited from aqueous solutions, this side reaction reduces the current efficiency and may even lead to cracks and low-quality products [2,3].

Recently, deep eutectic solvents (DESs), a class of room temperature ionic liquids, have emerged as promising non-aqueous electrolyte solutions for thin film electrodeposition applications due to their low cost, atmospheric stability, thermal stability, low toxicity, ability to dissolve metal salts, and relatively high conductivity [4,5]. The term DES refers to eutectic salt mixtures: usually, DESs consist of a quaternary ammonium salt (halide salt) and a metal salt or hydrogen bond donor (HBD). Their physical properties depend on the HBD and can be tailored to specific applications: removal of glycerol from biodiesel [6], processing of metal oxides [7], metal extraction [8], and synthesis of cellulose derivatives [9]. The use of DESs can offset the major drawbacks of aqueous electrodeposition processes, namely the narrow electrochemical window of water and the hydrogen evolution. DESs present wide electrochemical windows, which allow more control over nucleation and deposition rates and, in turn, affect the crystal grain size [10]. Further, their use theoretically precludes hydrogen evolution during electrodeposition due to the absence of water from

the system [11]. Therefore, non-aqueous electrodeposition may lead to higher quality deposits and could allow metals, such as Mn, to be incorporated into electrodeposited Fe alloys [12].

The aim of the current work was to investigate the electrodeposition of Fe and Fe–Mn alloys from a choline chloride (ChCl)/ethylene glycol (EG) DES. The effects of reduction potential and bath composition on the electrodeposition of Fe and Fe–Mn alloys were studied; the electrodeposition of this group of alloys is extremely challenging in aqueous solutions.

2. Materials and Methods

2.1. Electrolyte Preparation

ChCl ($\text{HOC}_2\text{H}_4\text{N}(\text{CH}_3)_3\text{Cl}$, 99%, Alfa Aesar, Ottawa, ON, Canada) and $\text{FeCl}_2 \cdot 4\text{H}_2\text{O}$ (99%, Acros Organics, Geel, Belgium) were placed in a vacuum chamber for 24 h at 60 °C to remove moisture before use. EG (anhydrous 99.8%, Sigma Aldrich, Hamilton, ON, Canada) and MnCl_2 (99%, Acros Organics, Geel, Belgium) were used as received. The DES was prepared by mixing and stirring dried ChCl with EG at a 1:2 molar ratio, at 90 °C, until a homogeneous colorless liquid was formed. Appropriate quantities of the metal salts were added to the DES, and the mixtures were stirred until homogeneous electrolyte solutions were obtained. The salt concentrations studied are shown in Table 1.

Table 1. Composition of the three electrolytes studied.

Chemical/Concentration (M)	S1	S2	S3
$\text{FeCl}_2 \cdot 4\text{H}_2\text{O}$	2.0	1.5	1.0
MnCl_2	0	0.5	1.0

2.2. Cyclic Voltammetry and Electrodeposition

Cyclic voltammetry (CV) experiments were carried out at 80 °C in a three-electrode cell (100 mL capacity). The system consisted of a glassy carbon (GC) working electrode, a GC counter electrode, and a pure silver quasi-reference electrode. A potential range from +2.0 V to −2.0 V was scanned at 20 mV/s.

The electrodepositions were performed using chronoamperometry analysis. The experiments were performed with a duration of 30 min using the same counter and reference electrodes as CV. The working electrode was a resin-mounted titanium sheet (1 cm × 1 cm area). The electrode surface was polished with a 1200 SiC paper before its use.

A Potentiostat/Galvanostat Versastat 3 was used to perform the electrochemical tests. The deposited materials were separated from the working electrode, rinsed with ethanol, and dried. A constant temperature of 80 °C was maintained throughout the electrodeposition tests. A potential of −1.35 V was applied for the three studied solutions.

2.3. Deposits Morphology and Composition

The surface morphology of the deposits was examined using a scanning electron microscope (FEI QUANTA 250) coupled with an energy dispersive X-ray (EDX) system. An accelerating voltage in the range 15 to 30 kV and a tungsten filament were used for the analyses. To evaluate the element amount and distribution, EDX was carried out at three points on the surface of each sample and an average value was obtained.

3. Results and Discussion

3.1. Cyclic Voltammetry (CV)

CV was applied to identify the potential window of the studied DES (Figure 1a), which defines the electrochemical stability of the solvents; the electrochemical window of ChCl/EG was circa. 3.0 V. Figure 1b presents a voltametric study carried out based on the individual response of the ChCl/EG DES with $\text{FeCl}_2 \cdot 4\text{H}_2\text{O}$ and MnCl_2 addition. Two cathodic branches were observed: C_1 (circa. 0.2 V) and C_2 (circa. −1.0 V), which may be

attributed to the reduction in Fe(III)/Fe(II) and the reduction in Fe(II)/Fe⁰ and Mn(II)/Mn⁰, respectively. Further, the addition of MnCl₂ was found to decrease the cathodic current. Similarly, two anodic peaks were detected: A₁ (+0.6 V), which is related to the oxidation of the Fe⁰/Fe(II), and A₂ (+1.4 V), which represents the oxidation of Fe(II)/Fe(III). The absence of an anodic process in the CV plots for Mn⁰/Mn(II) may be attributed to the instability of the manganese deposits, which are readily oxidized in the DES [13]. These observations are consistent to Panzeri et al. [14], who used a platinum wire as the reference electrode in their non-aqueous electrodeposition study of Fe from EG-based solvents.

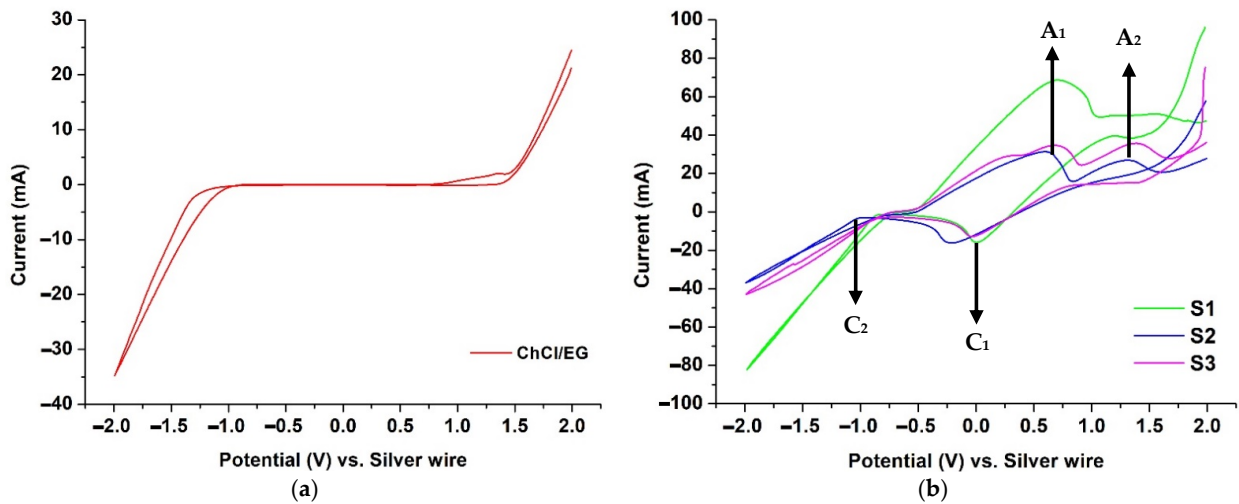


Figure 1. Cyclic voltammograms of (a) pure DES and (b) Fe and Fe–Mn bath electrolytes performed at 80 °C and 20 mV/s.

3.2. Chronoamperometry

To analyze the nucleation mechanism, chronoamperometric tests were performed. Figure 2 shows the current–time curves obtained for the deposition of Fe and Fe–Mn. The curves presented three stages corresponding to the metal nucleation process: the electric double layer charging (Part I), the formation and growth of Fe and Fe–Mn nuclei (Part II), and the metallic ion diffusion from the electrolyte to the electrode–solution interface (Part III) [15]. It was observed that solution S1 presented the highest deposition current compared to solutions S2 and S3.

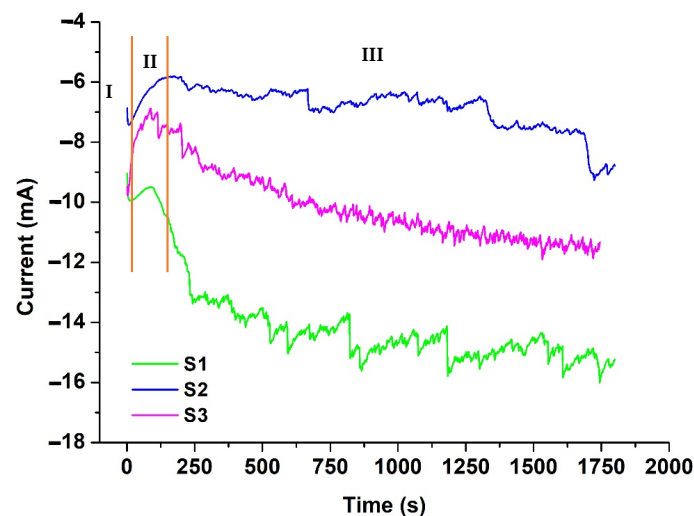


Figure 2. Experimental current density transients recorded during the electrodeposition onto the titanium substrate from the system ChCl/EG with Fe and Mn salt addition at 80 °C.

3.3. Film Morphology and Microstructure

Scanning electron microscopy (SEM) was performed to study the surface morphology of the electrodeposited pure Fe (Figure 3a) and Fe–Mn alloys (Figure 3b,c). A thin layer appeared to detach from the surface of the pure Fe deposit, which may be related to the high current deposition observed in the chronoamperometry curves. The island-shaped surface morphology showed features with an average diameter (or main dimension) larger than 5.0 μm . With the addition of MnCl_2 (0.5 M) (Figure 3b), a dense and uniform deposit composed of particles around 2.0–3.0 μm was obtained. Finally, upon the addition of MnCl_2 (1.0 M), the deposited surface was inhomogeneous and non-adherent (Figure 3c). Based on the atomic percent of Fe and Mn on the deposits obtained by EDX (Table 2), the amount of Mn in the electrolyte bath did not significantly change the final Fe–Mn alloy composition.

Table 2. Atomic percent of Fe and Mn in the three deposits obtained with EDX.

	Composition of the Deposit by EDX	
	Fe (at%)	Mn (at%)
S1	100	0
S2	97 ± 1.5	3 ± 1.5
S3	98 ± 0.1	2 ± 0.1

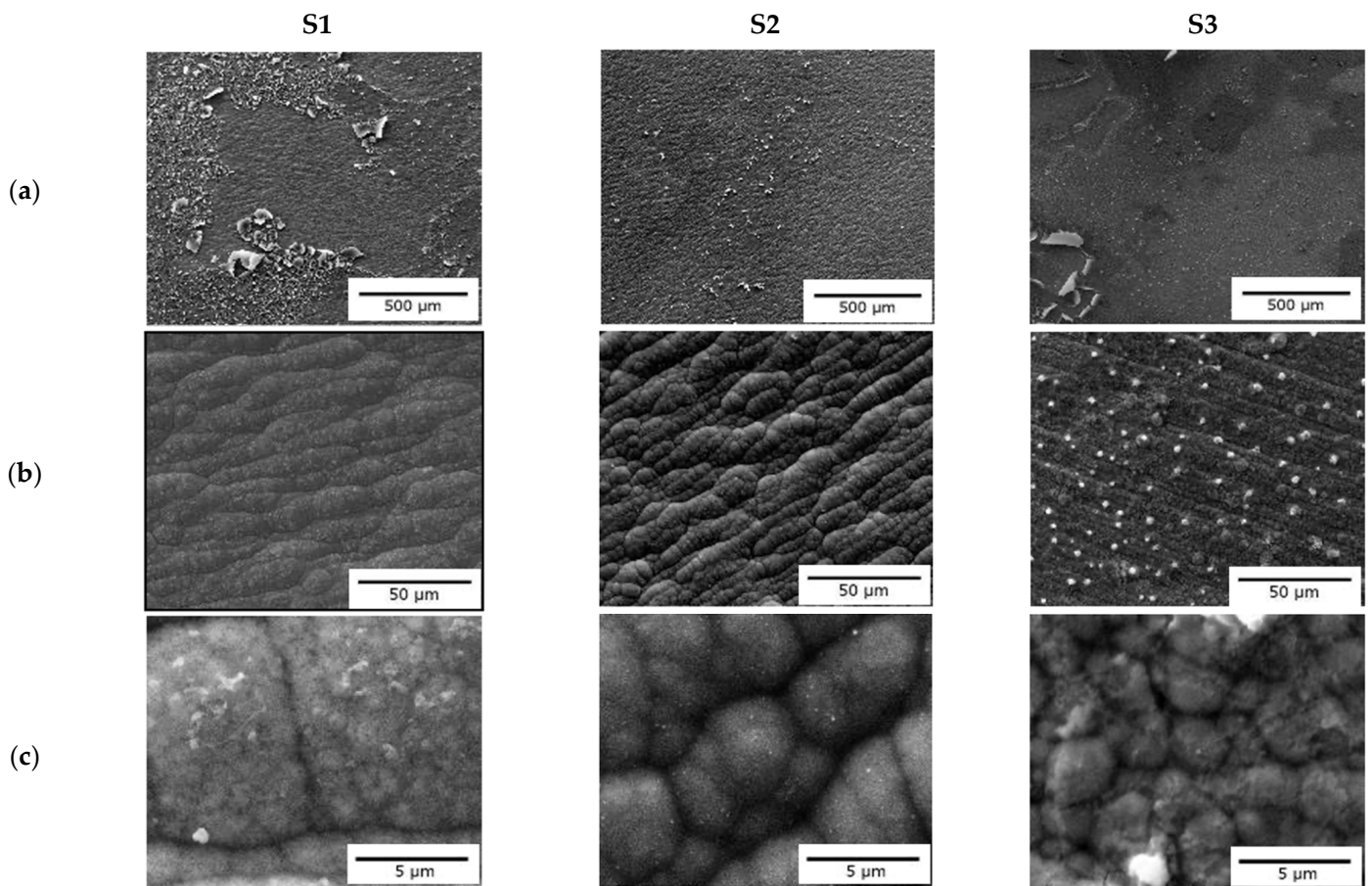


Figure 3. SEM images of the surface of deposits obtained for different concentrations of Fe–Mn and magnification of (a) 100 \times , (b) 1000 \times , and (c) 10,000 \times .

4. Conclusions

Fe–Mn alloys were electrodeposited from a choline chloride/ethylene glycol deep eutectic solvent. The cyclic voltammograms showed that the reduction process of Fe and Mn takes place inside the potential window of the DES. It was shown that the addition of Mn affects the current deposition of the Fe–Mn alloy. Although an increase in Mn concentration in the electrolyte bath did not produce deposits with high content of this element, the morphology of the deposits was affected. The addition of Mn decreased the size of the particles that form the deposition. Future steps involve the investigation of the effectiveness of this process for the fabrication of thin-walled devices.

Author Contributions: V.S. performed the analysis of CV, deposition, and SEM, contributed to the interpretation of results, and participated in the writing of the manuscript. C.P., D.M. and G.K. contributed to the interpretation of results and participated in the writing of the manuscript. All authors have read and agreed to the published version of the manuscript.

Institutional Review Board Statement: Not applicable.

Informed Consent Statement: Not applicable.

Data Availability Statement: The data presented in this study are available upon request from the corresponding author.

Acknowledgments: This work was funded by NSERC-Canada under the CU-I2I program. D.M. was supported by NSERC-Canada and holds a Canada Research Chair Tier I.

Conflicts of Interest: The authors declare no conflict of interest.

References

1. Yuliy, D.; Gamburg, G.Z. *Theory and Practice of Metal Electrodeposition*; Springer: New York, NY, USA, 2011; Volume 35, ISBN 9781441996688.
2. Andricacos, P.C.; Robertson, N. Future directions in electroplated materials for thin-film recording heads. *IBM J. Res. Dev.* **1998**, *42*, 671–680. [[CrossRef](#)]
3. Guo, J.; Guo, X.; Wang, S.; Zhang, Z.; Dong, J.; Peng, L.; Ding, W. Effects of glycine and current density on the mechanism of electrodeposition, composition and properties of Ni–Mn films prepared in ionic liquid. *Appl. Surf. Sci.* **2016**, *365*, 31–37. [[CrossRef](#)]
4. Endres, F. Ionic liquids: Solvents for the electrodeposition of metals and semiconductors. *ChemPhysChem* **2002**, *3*, 144–154. [[CrossRef](#)]
5. Simka, W.; Puszczczyk, D.; Nawrat, G. Electrodeposition of metals from non-aqueous solutions. *Electrochim. Acta* **2009**, *54*, 5307–5319. [[CrossRef](#)]
6. Abbott, A.P.; Cullis, P.M.; Gibson, M.J.; Harris, R.C.; Raven, E. Extraction of glycerol from biodiesel into a eutectic based ionic liquid. *Green Chem.* **2007**, *9*, 868–887. [[CrossRef](#)]
7. Abbott, A.P.; Capper, G.; Davies, D.L.; McKenzie, K.J.; Obi, S.U. Solubility of metal oxides in deep eutectic solvents based on choline chloride. *J. Chem. Eng. Data* **2006**, *51*, 1280–1282. [[CrossRef](#)]
8. Larsson, K.; Binnemans, K. Selective extraction of metals using ionic liquids for nickel metal hydride battery recycling. *Green Chem.* **2014**, *16*, 4595–4603. [[CrossRef](#)]
9. Abbott, A.P.; Bell, T.J.; Handa, S.; Stoddart, B. Cationic functionalisation of cellulose using a choline based ionic liquid analogue. *Green Chem.* **2006**, *8*, 784–786. [[CrossRef](#)]
10. Smith, E.L.; Abbott, A.P.; Ryder, K.S. Deep Eutectic Solvents (DESs) and Their Applications. *Chem. Rev.* **2014**, *114*, 11060–11082. [[CrossRef](#)] [[PubMed](#)]
11. Liu, F.; Deng, Y.; Han, X.; Hu, W.; Zhong, C. Electrodeposition of metals and alloys from ionic liquids. *J. Alloys Compd.* **2016**, *654*, 163–170. [[CrossRef](#)]
12. Sides, W.D.; Huang, Q. Electrodeposition of manganese thin films on a rotating disk electrode from choline chloride/urea based ionic liquids. *Electrochim. Acta* **2018**, *266*, 185–192. [[CrossRef](#)]
13. Pereira, N.M.; Soc, J.E.; Pereira, N.M.; Pereira, C.M.; Ara, P. Electrodeposition of Mn and Mn–Sn Alloy Using Choline Chloride-Based Ionic Liquids Electrodeposition of Mn and Mn–Sn Alloy Using Choline Chloride-Based Ionic Liquids. *J. Electrochem. Soc.* **2017**, *164*, D486. [[CrossRef](#)]
14. Panzeri, G.; Accogli, A.; Gibertini, E.; Rinaldi, C.; Nobili, L.; Magagnin, L. Electrodeposition of high-purity nanostructured iron films from Fe(II) and Fe(III) non-aqueous solutions based on ethylene glycol. *Electrochim. Acta* **2018**, *271*, 576–581. [[CrossRef](#)]
15. Kahoul, A.; Azizi, F.; Bouaoud, M. Effect of citrate additive on the electrodeposition and corrosion behaviour of Zn–Co alloy. *Trans. Inst. Met. Finish.* **2017**, *95*, 106–113. [[CrossRef](#)]